Near-stoichiometric Ti:$LiNbO_3$ strip waveguide with varied substrate refractive index in waveguide layer*

Zhang De-Long(张德龙)[a)b)†], Wu Chang(吴 嫦)[a)], and Pun Edwin Yue-Bun(潘裕斌)[b)]

[a)] *School of Precision Instruments and Opto-electronics Engineering, Tianjin University, Tianjin* 300072, *China, and Key Laboratory of Optoelectronics Information Science and Technology, Ministry of Education, Tianjin* 300072, *China*

[b)] *Department of Electronic Engineering, City University of Hong Kong, 83 Tat Chee Avenue, Kowloon, Hong Kong SAR, China*

(Received 18 November 2008; revised manuscript received 10 September 2009)

We report the near-stoichiometric Ti:$LiNbO_3$ strip waveguides fabricated by vapour transport equilibration (VTE) at 1060 °C for 12 h and co-diffusion of 4–8 μm wide, 115-nm thick Ti-strips. Optical studies show that these waveguides are monomode at 1.5 μm and have losses of 1.3 and 1.1 dB/cm for the TM and TE modes, respectively. In the waveguide width/depth direction, the mode field follows a Gauss/Hermite–Gauss profile. A secondary ion mass spectrometry study reveals that the Ti profile follows a sum of two error functions along the width direction and a complementary error function in the depth direction. Micro-Raman analysis shows that the Li-composition in the depth direction also follows a complementary error function. The mean Li/Nb ratio in the waveguide layer is about 0.98. The inhomogeneous Li-composition profile results in a varied substrate index in the guiding layer, and the refractive index profile in the guiding layer is given.

Keywords: near-stoichiometric Ti:$LiNbO_3$ strip waveguide, varied substrate refractive index, Li-composition profile, 2D refractive index profile

PACC: 4280L, 4282

1. Introduction

Although a near-stoichiometric $LiNbO_3$ displays higher photorefractive sensitivity than a congruent material within continuous-wave intensity,[1] a near-stoichiometric Ti:$LiNbO_3$ waveguide may find applications in the wavelength range from 1.5 μm to mid-IR, where the photorefractive effect is relatively weak. Recently, we have reported single-mode near-stoichiometric Ti:$LiNbO_3$ strip waveguides fabricated by co-work of vapor transport equilibration (VTE) treatment at 1100 °C and thermal diffusion of Ti-metal strips.[2] To ensure the Li-composition over the whole substrate being homogeneous and near-stoichiometric, a very long VTE duration of 101 h was adopted for the fabrication of those waveguides. For a practical Ti:(Er:)$LiNbO_3$ device, both the waveguide and the Er-doped layers are defined on the crystal surface with a 1/e concentration depth of only several microns. There is no need to adopt very long VTE duration to render the whole substrate being fully VTE-treated. Shorter VTE duration may render the guiding layer near-stoichiometric. Here, we report single-mode (at 1.5 μm) near-stoichiometric Ti:$LiNbO_3$ strip waveguides that were fabricated under a much weak VTE strength (1060 °C/12 h). The waveguides fabricated under such a weak VTE condition have an inhomogeneous Li-composition profile along the depth direction. Since the refractive index of the $LiNbO_3$ crystal is Li-composition-dependent,[3,4] the waveguide fabricated is of varied substrate index in the guiding layer.

Note that the nomenclature "Li-composition" has a different meaning from the "Li-concentration". The former means the stoichiometry of Li in a $LiNbO_3$ molecule. While the latter, in unit of ions/cm^3, means Li ion number per unit volume. In a congruent $LiNbO_3$ crystal, for example, the Li stoichiometry is 0.945, and all of the Li ions in a $LiNbO_3$ crystal occupy the regular Li lattice sites. The Li-concentration can be easily converted from the Li stoichiometry by simply multiplying by a factor of 1.85×10^{22} ions/cm^3. On the other hand, if not all of the Li ions occupy the regular Li lattice sites (for example, in some specific case, part of Li ions may occupy the Nb sites), the Li-composition and the Li-concentration no longer follow such a simple conversion relationship.

*Project supported by the National Natural Science Foundation of China (Grant Nos. 50872089 and 60577012) and the Research Grants Council of the Hong Kong Special Administrative Region, China (Grant No. CityU 1194/07).

†Corresponding author. E-mail: delongzhang@eyou.com

© 2010 Chinese Physical Society and IOP Publishing Ltd

2. Experimental

In total five groups of Ti strips were fabricated. The initial Ti-strip thickness was 115 nm and the initial Ti-strip width W was 4, 5, 6, 7 and 8 μm. All of the Ti-strips were photolithographically patterned on one surface of a 1-mm thick Z-cut [i.e. (001) face] congruent substrate. Each group included five same Ti-strips. After the Ti-strip was patterned, the Li-rich VTE treatment[2] was carried out for the substrate at 1060 °C for 12 h.

To facilitate the end-fire coupling experiment and the subsequent micro-Raman analysis, the two endfaces of the sample were optically polished after the VTE treatment. The final length of the waveguide is $\sim$ 1.5 cm. The end-fire experiment was carried out by launching into the waveguides the polarised 1.5-μm light emitted from a fiber-pigtailed superfluorescence light emitting diode with a band width of 1510–1590 nm via endface butt-coupling between a polarisation-maintaining fiber and the channel waveguide. A polarisation controller (Optics for Research Inc.) was used to control the state of polarisation of the light launched into the waveguide. The magnified near-field image of the guided TE or TM mode was projected onto an infrared Hamamatsu digitizing video camera (Vidicon 1000) through a Nikon microscope objective lens with a magnification of 50×, a working distance of 1 mm and a numerical aperture of 0.8. The insertion losses of the waveguides were measured using a 1.55-μm semiconductor distributed feedback laser diode with an output power of 2.5 dBm.

Secondary ion mass spectrometry (SIMS) was used to analyse the concentration profiles of the indiffused Ti ions in the depth direction and on the surface of the 6-μm wide strip waveguide. The surface Ti concentration profile was analysed by a PHI-7200 (Physical Electronics) time-of flight secondary ion mass spectrometer. A 25-keV Ga^+ beam with a diameter of 0.5 μm was used to raster a 250×250 μm^2 area and the secondary Ti ions were mapped. The total ion dose is $\sim 4\times10^{12}$ ions/cm^2. The lateral resolution is about 0.5 μm. The depth profile of Ti-concentration was analysed by a time-of-flight secondary ion mass spectrometer (TOF SIMS V, ION-TOF GmbH). An O_2^+-beam was used to sputter a crater of 100×100 μm^2 and the positive secondary ions of $^{93}Nb^+$, $^{16}O^+$, $^7Li^+$ and $^{48}Ti^+$ were recorded as functions of time. Ions from a central area of 3 μm in diameter inside the crater were detected, so that the SIMS signals detected are mainly from the waveguide. During the analysis, a normal incidence electron gun, equipped in the TOF SIMS V system, was used to compensate the surface charge accumulation. The total sputtering time is 3.0×10^4 second. The depth of the erosion crater was measured by a profilometer Tencor Alpha Step 200. The depth resolution is mainly determined by the roughness of the crater under analysis, being $\sim$ 50 nm.

The 153-cm^{-1} phonon linewidth method[5] was used to determine the depth profile of the Li-composition in the 6-μm wide waveguide layer. Micro-Raman analysis was performed on one waveguide endface by using a Jobin–Yvon T64000 confocal microscope Raman spectrometer. The T64000 system not only has a higher spectral resolution ($\sim$ 0.1 cm^{-1}), but also possesses other two intrinsic advantages. The diameter of the analyzable area can be as small as $\sim$ 1 μm. Such a probe area is so small that can be used to analyse the strip waveguides with the width of several microns. It is more important that the excitation position and the scattering light collection position are confocal. The sample was arranged on a translation slide (with an accuracy of 3 μm), and the sample could be moved laterally. The 488-nm line (150 mW) emitted from an INNOVA 705 argon laser was used as the excitation source. The polarised excitation light was focused onto the sample through a 100× objective of microscope, under which the diameter of the excitation beam was $\sim$ 1 μm. However, due to Rayleigh scattering effect, the depth of focus of such a focused 488-nm laser spot in $LiNbO_3$ crystal will extend to $\sim$ 7 μm, which is considerably larger than the Ti-penetration depth ($\sim$ 2.6 μm) and Li diffusion depth ($\sim$ 3.64 μm). Since the confocally collected Raman signal is an average over the depth of focus, the scattering configuration should be chosen carefully to minimize the influence of the depth of focus to a largest extent. Here, the backward scattering geometry $Y(ZX)\bar{Y}$ was adopted. The excitation light was oriented along the strip waveguide (i.e. along the Y crystallographic axis of the crystal). In such a scattering configuration, the measurement was not influenced by the Rayleigh effect and the crystal surface could be clearly identified. The Raman analysis on the waveguide endface was carried out point by point along the depth direction. The recorded spectra are pure E(TO) phonons. All Raman measurements were carried out at room temperature in the wavenumber range of 100–1000 cm^{-1}. The time used for the record of each spectrum lasted 60 s. For comparison, the micro-Raman analysis was also performed

on the Ti-free area. In addition, to quantitatively evaluate the Ti-concentration-dependent broadening of the 153-cm^{-1} phonon arising from the Ti-dopant, the same micro-Raman analysis was also carried out on fine polished endface of a standard congruent Z-cut Ti:$LiNbO_3$ strip waveguide, fabricated by in-diffusion of 6-μm wide, 95-nm thick Ti strip at 1030 °C for 9 h in an argon atmosphere.

3. Results and discussion

After the VTE treatment, the strip waveguides were checked by an optical microscope, and the surfaces are found to be smooth and flat as shown in Fig. 1, where, as an example, an image of a 6-μm wide strip waveguide is shown. It was found that waveguiding was observed for all waveguides under both TM and TE polarisations, and all waveguides are single-mode. The insets in Fig. 1 show the TM and TE mode patterns of the 6-μm wide waveguide. Note that the size of the TE mode is significantly larger than that of the TM mode. Figure 2 shows the light intensity profiles (full squares) along the width (x) and depth (y) directions for the TM and TE modes respectively in the 6-μm wide waveguide. Along the x direction, the profiles of both TM and TE modes can be well fitted by a Gauss trial function $\exp(-2x^2/W_x^2)$ (see solid curves in Figs. 2(a) and 2(c)). In the y direction, the profiles follow a Hermite–Gauss function $A_0 y^2 \exp(-2y^2/W_y^2)$ [see solid curves in Figs. 2(b) and 2(d)]. The mode size W_x (W_y) is about 3.5 (4.4) $\pm$ 0.2 μm for the TM mode and 5.6 (5.3) $\pm$ 0.2 μm for the TE mode.

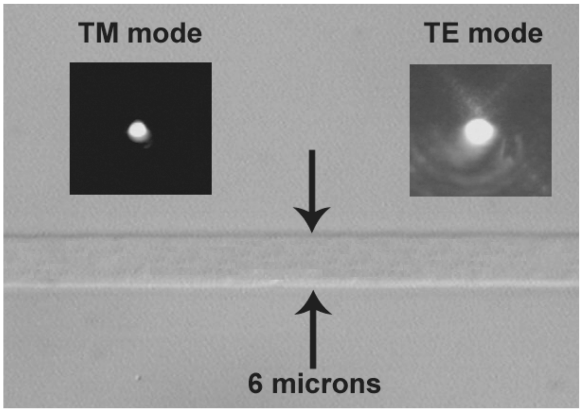


Fig. 1. Image of near-stoichiometric Ti:$LiNbO_3$ strip waveguide with initial Ti-strip width of 6 μm. Images attached show TM- and TE-polarised single-mode near-field patterns of the waveguide at 1.5 μm.

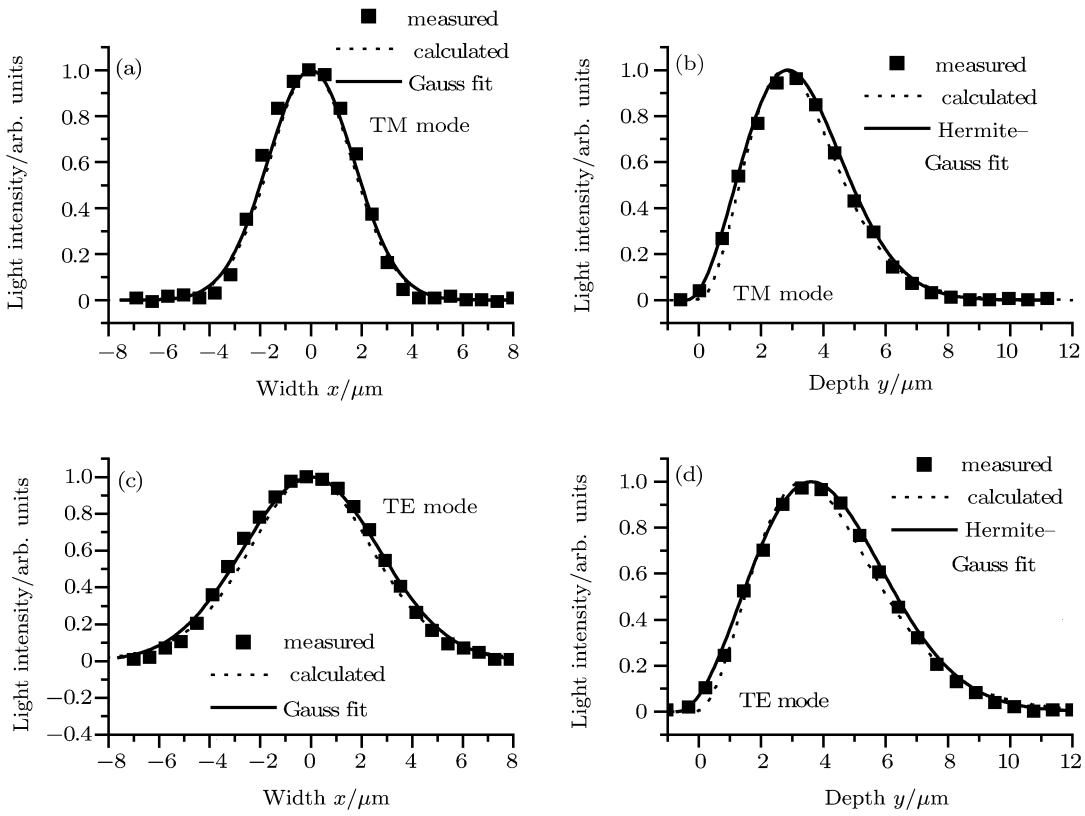


Fig. 2. TM- and TE-polarised light intensity profiles (full squares) along the width and depth directions of the 6-μm wide near-stoichiometric strip waveguide. The solid curves represent the fitting results and the dotted curves the BPM simulation results.

The average fibre-to-fibre insertion loss of five waveguides (each being 1.5-cm long and 6-μm wide) was evaluated to be 6.2 dB for the TM mode and 4.4 dB for the TE mode. From the measured mode sizes, the coupling loss between the 6-μm wide waveguide and a single-mode fibre (with a mode field diameter of 10 μm) is about 2.0 dB for the TM mode and 1.2 dB for the TE mode. With etalon effect ignored, the total Fresnel reflection loss of the two waveguide endfaces against the two fibre endfaces is about 0.27 and 0.33 dB for the TM and TE polarisations, respectively. The propagation loss is then evaluated to be smaller than 1.3 dB/cm for the TM mode and 1.1 dB/cm for the TE mode, and shows slight polarisation dependence. The waveguide loss of the usual congruent Ti:$LiNbO_3$ strip waveguide shows similar polarisation dependence.[6] This optical characteristic may be qualitatively explained as follows: for a fundamental mode that is guided in a straight Ti:$LiNbO_3$ waveguide, its propagation loss is mainly contributed from the background absorption of the substrate material itself and the scattering loss. The background absorptions include the interband (from valence band to conduction band) electron resonance absorption and the lattice vibration absorption. For the $LiNbO_3$ crystal, the electron resonance occurs in the ultra-violet region ($\lambda < 0.4$ μm), while the lattice vibration absorption takes place in the far infrared region ($\lambda > 11$ μm). The tails of these absorptions extend to the visible and near infrared regions, where an optical waveguide device usually works. In addition, for the $LiNbO_3$ crystal, the background absorption includes also the contribution from the OH^- group ($\sim$ 2.865 μm or 3490 cm^{-1}). All of these absorption processes should be of the polarisation dependence due to the anisotropy of the $LiNbO_3$ crystal. For a TM (TE)-polarised light wave that is guided in a Z-cut $LiNbO_3$ crystal, the electric field involved is parallel (perpendicular) to the optical axis of the crystal and the refractive index involved is n_e (n_o). Due to the anisotropy of the crystal, the background absorption should be different for the TM and TE waves. The scattering loss usually includes two contributions: Rayleigh scattering and Mie scattering. The former is a fundamental loss mechanism arising from local microscopic fluctuations in medium density. The density fluctuations lead to random fluctuations of the refractive index on a scale smaller than the optical wavelength. The Rayleigh scattering loss varies as $1/\lambda^4$. The Mie scattering is conducted with the imperfection of the waveguide. It occurs mainly due to the index inhomogeneity on a scale longer than the optical wavelength. Because the scattering is the radiation of electromagnetic wave in nature, both the Rayleigh scattering and the Mie scattering can be considered as the conversion of the guided mode to the radiation mode. Since the definition of the scattering cross section is associated with the density of the energy flow of the scattered wave, and the field of the scattered wave is solved from a complicated integration equation that is associated with the dielectric permittivity of the scatter, which is of the anisotropy for the $LiNbO_3$, so the scattering loss is also polarisation-dependent.

Figure 3(a) shows the SIMS profile (full squares) of Ti-concentration on the surface of the 6-μm wide waveguide. One can see from Fig. 3(a) that the experimental data can be well fitted by the sum of two error functions. The diffusion width d_x is about 3.8 μm.

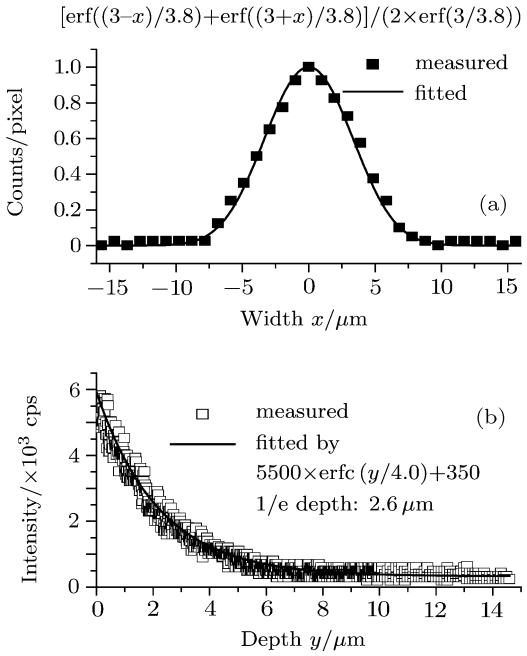


Fig. 3. (a) Measured SIMS profile (full squares) of Ti-concentration along the width direction of the 6-μm wide near-stoichiometric Ti:$LiNbO_3$ strip waveguide. (b) Measured depth profile (open squares) of Ti-concentration of the same strip waveguide. The solid curves in (a) and (b) represent the fitting results.

Figure 3(b) shows the depth profile of the Ti SIMS signals from the same waveguide. One can see that the depth profile can be well fitted by a complementary error function

$$C_{\mathrm{Ti}}(y) = C_0 \mathrm{erfc}(y/d_y). \quad (1)$$

The parameter d_y is about 4.0 μm, which corresponds to a 1/e diffusion depth of 2.6 μm. The two-dimensional Ti-concentration profile in the waveguide

is given by

$$C_{\mathrm{Ti}}(x,y) = C_0 \frac{1}{2\mathrm{erf}\left(\dfrac{W}{2d_x}\right)} \left[\mathrm{erf}\left(\frac{W+2x}{2d_x}\right) + \mathrm{erf}\left(\frac{W-2x}{2d_x}\right)\right] \mathrm{erfc}(y/d_y). \quad (2)$$

By applying the law of mass conservation to Eq. (2), the surface Ti-concentration C_0 is determined to be 3.0×10^{21} ions/cm^3, equivalent to ~ 16 mol%.

Since the Li_2O content change from the congruent point (48.4 mol%) to the ideal stoichiometric composition (50 mol%) is only 1.6 mol%, the SIMS analysis cannot give a reliable result on the Li-concentration profile. Speaking strictly, the substrate refractive index in the guiding layer depends on the Li-composition instead of the Li-concentration. So, it is more important to know the Li-composition profile. Here, the 153-cm^{-1} phonon linewidth method[5] was employed to determine the depth profile of the Li-composition in the 6-μm wide waveguide layer. Micro-Raman analysis was performed on endfaces of the VTE waveguide studied here and a standard congruent waveguide. The fabrication parameters of the standard congruent waveguide were intentionally chosen to be the same as those reported in Ref. [6], so that the Ti-concentration profile reported in that paper can be directly utilized. The Raman study of the congruent waveguide allows to fix Ti-induced broadening of the 153-cm^{-1} phonon, Γ_0, as a function of the Ti-concentration ($\Gamma_0 = 0.351 C_{\mathrm{Ti}}$). Then, the Li-composition-related 153-cm^{-1} phonon [E(TO)] FWHM (Γ) profile along the depth direction of the VTE waveguide can be obtained by subtracting the Γ_0 from the measured total phonon FWHM data of the VTE waveguide. The results are shown in Fig. 4(a), from which the Li-composition profile along the depth direction of the VTE waveguide can be evaluated using the empirical relation reported by Malovichko *et al.*[5] It was found that the expression reported by Malovichko *et al.* needs to be modified slightly on the basis of their experimental data. The modified expression is $C_{\mathrm{Li_2O}}[\mathrm{mol\%}] = 52.52757 - 0.41131\Gamma[\mathrm{cm}^{-1}]$. Figure 4(b) shows the obtained depth profile of the ([$\mathrm{Li_{Li}}$]+[$\mathrm{Ti_{Li}}$])/([$\mathrm{Nb_{Nb}}$]+[$\mathrm{Ti_{Nb}}$]) ratio (open circle). The ([$\mathrm{Li_{Li}}$]+[$\mathrm{Ti_{Li}}$])/([$\mathrm{Nb_{Nb}}$]+[$\mathrm{Ti_{Nb}}$]) ratio results from the assumption that the Ti ions incorporated occupy both Nb and Li sites. The solid line represents a fit to the experimental data by using a complementary trial function erfc(y/d) with $d = 5.7$ μm. Note that the Li-composition at the waveguide surface can be considered as stoichiometric within the experimental error of ± 0.002. The averaged ([$\mathrm{Li_{Li}}$]+[$\mathrm{Ti_{Li}}$])/([$\mathrm{Nb_{Nb}}$]+[$\mathrm{Ti_{Nb}}$]) ratio over the waveguide layer (0–2.6 μm) is about 0.98, close to stoichiometric composition. The 1/e depth is about 3.64 μm, considerably larger than the 1/e Ti diffusion depth, ~ 2.6 μm. The inhomogeneous Li-composition results in varied substrate index in the waveguide

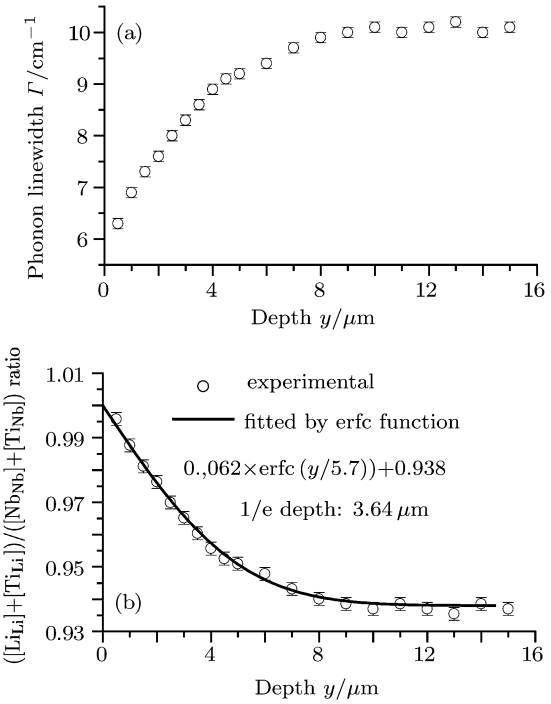


Fig. 4. (a) Depth profile of Li-composition-related 153-cm^{-1} phonon broadening Γ in VTE Ti:$LiNbO_3$ strip waveguide. (b) Depth profile of ([$\mathrm{Li_{Li}}$]+[$\mathrm{Ti_{Li}}$])/([$\mathrm{Nb_{Nb}}$]+[$\mathrm{Ti_{Nb}}$]) ratio (open circle) obtained from 4(a).

layer. From Fig. 4(b), the substrate indices in the waveguide layer, $n_{\mathrm{eb}}(y)$ and $n_{\mathrm{ob}}(y)$, can be readily calculated from the Li_2O-content-dependent Sellmeier equations,[3] and are shown in Fig. 5. Both the extraordinary and ordinary substrate index profiles can be well fitted still by a complementary error function

$$n_{\mathrm{eb}}(y) = n_{\mathrm{e}}^{\mathrm{cLN}} + (n_{\mathrm{e}}^{\mathrm{sLN}} - n_{\mathrm{e}}^{\mathrm{cLN}}) \cdot \mathrm{erfc}(y/d_{\mathrm{e}}), \quad (3)$$

$$n_{\mathrm{ob}}(y) = n_{\mathrm{o}}^{\mathrm{cLN}} + (n_{\mathrm{o}}^{\mathrm{sLN}} - n_{\mathrm{o}}^{\mathrm{cLN}}) \cdot \mathrm{erfc}(y/d_{\mathrm{o}}), \quad (4)$$

where $n_{\mathrm{e,o}}^{\mathrm{cLN}}$ and $n_{\mathrm{e,o}}^{\mathrm{sLN}}$ are the indices at the congruent (48.4 mol%) and stoichiometric (50 mol%) composition, respectively; and $d_{\mathrm{e,o}}$ is the profile parameter having the same value of 5.6 μm in both cases.

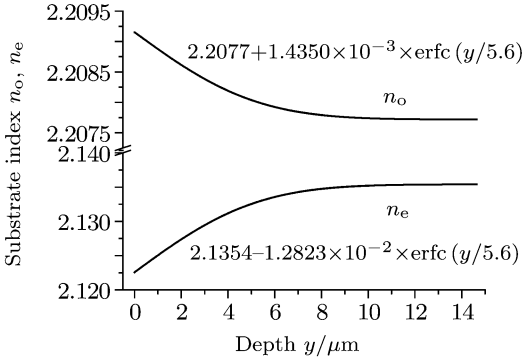


Fig. 5. Depth profiles of substrate refractive index n_e and n_o at 1545-nm wavelength.

Nakamura *et al.*[7] have reported that both the ordinary and extraordinary refractive index changes induced by Ti dopant in *bulk* Ti-doped near-stoichiometric $LiNbO_3$ crystal increase linearly with Ti-concentration. In parallel, Hellwig *et al.*[8] have reported similar result on near-stoichiometric MgO:Ti:$LiNbO_3$ planar waveguides. Assume this linearity is also valid for our near-stoichiometric waveguide here. Based upon Eq. (2), the profile of Ti-induced refractive index change in the near-stoichiometric strip waveguide can be expressed as

$$\Delta n_{\mathrm{e,o}}(x,y) = \Delta n(0,0)_{\mathrm{e,o}} \frac{1}{2\mathrm{erf}\left(\dfrac{W}{2d_x}\right)} \left[\mathrm{erf}\left(\frac{W+2x}{2d_x}\right) + \mathrm{erf}\left(\frac{W-2x}{2d_x}\right)\right] \mathrm{erfc}(y/d_y), \tag{5}$$

where $\Delta n_{\mathrm{e,o}}(0,0)$, abbreviated as $\Delta n_{\mathrm{e,o}}$ for convenience, is the Ti-induced extraordinary or ordinary refractive index increment at $x = y = 0$. By combining Eqs. (3)–(5) and ignoring small terms, the extraordinary and ordinary refractive index profiles, $n_e(x,y)$ and $n_o(x,y)$, in the near-stoichiometric strip waveguide layer can be approximated as

$$n^2_{\mathrm{e,o}}(x,y) \approx \begin{cases} 1, & y < 0, \\ (n^{\mathrm{cLN}}_{\mathrm{e,o}})^2 + 2n^{\mathrm{cLN}}_{\mathrm{e,o}}(n^{\mathrm{sLN}}_{\mathrm{e,o}} - n^{\mathrm{cLN}}_{\mathrm{e,o}}) \cdot \mathrm{erfc}(y/d_{\mathrm{e,o}}) + 2n^{\mathrm{cLN}}_{\mathrm{e,o}}\Delta n_{\mathrm{e,o}}(x,y), & y \geq 0. \end{cases} \tag{6}$$

From the Ti surface concentration given above and the linear relationships of the Δn_o and Δn_e with the Ti-concentration,[7] Δn_o (1545 nm) and Δn_e (1545 nm) of our near-stoichiometric waveguide are evaluated to be 0.01 and 0.034, respectively. On the other hand, one can see from Fig. 5 that the index change due to the Li-composition alteration is about –0.0128 and 0.0014 for the extraordinary and the ordinary rays, respectively. The net index increments are thus 0.0212 and 0.0114, respectively, showing that our near-stoichiometric strip waveguide confines a TM mode more effectively than a TE mode. This is qualitatively consistent with the experimental result shown in Fig. 1.

Based on Eq. (6), we have calculated the fundamental mode field profiles using the 3D beam propagation method (BeamPROP from RSoft Design Group, Inc.). The calculated results are shown in Fig. 2 (see dotted curves). One can see that the numerical results are essentially in agreement with the experimental data. This means that the refractive index model proposed is close to the real scenario.

4. Conclusion

We have demonstrated that near-stoichiometric Ti:$LiNbO_3$ strip waveguides can be fabricated by carrying out VTE treatment at 1060 °C for 12 h on congruent $LiNbO_3$ substrate with photolithographically defined 4–8 μm wide, 115-nm thick Ti-strips. Optical studies show that all of these waveguides are single-mode at 1.5 μm and the waveguide loss is lower than 1.3 dB/cm for TM mode and 1.1 dB/cm for TE mode. In the width/depth direction of the waveguide, the mode field follows the Gauss/Hermite–Gauss function. The Ti ions along the width and depth directions of the waveguide follow a sum of two error functions and a complementary error function profile, respectively. The surface Ti-concentration, 1/e width and depth are 3.0×10^{21} cm^{-3}, 3.8 μm and 2.6 μm, respectively. The depth profile of Li-composition in the waveguide layer also follows a complementary error function with a 1/e depth of 3.64 μm. The mean $([\mathrm{Li_{Li}}]+[\mathrm{Ti_{Li}}])/([\mathrm{Nb_{Nb}}]+[\mathrm{Ti_{Nb}}])$ ratio in the waveguide layer is about 0.98. The inhomogeneous Li-composition profile results in a varied substrate refractive index in the guiding layer. The

two-dimensional refractive index profile model is proposed for the near-stoichiometric strip waveguide by taking into account the varied substrate index and assuming the linearity between the Ti-induced index change and Ti-concentration. The Ti-induced waveguide surface refractive index increments at 1545 nm, $\Delta n_{\rm o}$ and $\Delta n_{\rm e}$, are evaluated to be 0.01 and 0.034, respectively, and the net waveguide surface increments are about 0.0114 and 0.0212, respectively. Agreement between the theoretical results and the experimental data indicates that the refractive index profile model proposed is close to the practical scenario.

Near-stoichiometric waveguides fabricated using the present method have the advantage of the absence of the Li out-diffusion problem and more free single-mode condition over the usual congruent Ti:$LiNbO_3$ waveguides. Moreover, the feature of the varied substrate index in the guiding layer may offer the possibility of tailoring the waveguide properties through the controllable VTE parameters, initial Ti-strip width and thickness. With an optimized photolithographic procedure, initial Ti-strip thickness and VTE parameters, the near-stoichiometric waveguides would be of a lower loss level as a result of the reduction of the intrinsic defects inside the crystal.

References

[1] Jermann F, Simon D M and Kratzig E 1995 *J. Opt. Soc. Am.* B **12** 2066

[2] Zhang D L, Wong W H and Pun E Y B 2004 *Appl. Phys. Lett.* **85** 3002

[3] Schlarb U and Betzler K 1993 *Phys. Rev.* B **48** 15613

[4] Jundt D H, Fejer M M and Byer R L 1990 *IEEE J. Quantum Electron.* **26** 135

[5] Malovichko G I, Grachev V G, Kokanyan E P, Schirmer O F, Betzler K, Gather B, Jermann F, Klauer S, Schlarb U and Wohlecke M 1993 *Appl. Phys.* A: *Solids & Surf.* **56** 103

[6] Baumann I, Brinkmann R, Dinand M, Sohler W and Westenhöfer S 1996 *IEEE J. Quantum Electron.* **32** 1695

[7] Nakamura M, Takekawa S, Kurimura S, Kitamura K and Nakajima H 2004 *J. Crystal Growth* **264** 339

[8] Hellwig A, Suche H, Schor R and Sohler W "*Titanium-indiffused Waveguides in Magnesium Oxide Doped Stoichiometric Lithium Niobate* (MgO:SLN)," *12th European Conference on Integrated Optics* (ECIO'05), Grenoble, France, ThB2-5, 2005